J Nanopart Res (2012) 14:652
DOI 10.1007/s11051-011-0652-0

RESEARCH PAPER

Plasmonic properties of two-dimensional metallic nanoholes fabricated by focused ion beam lithography

Shaoli Zhu · Wei Zhou

Received: 12 July 2011 / Accepted: 22 December 2011 / Published online: 14 February 2012

Abstract Plasmonic metallic nanoholes are widely used to focus or image in the nanoscale field. In this article, we present the results of the design, fabrication, and plasmonic properties of a two-dimensional metallic pentagram nanohole array. The nanoholes can excite the extraordinary transmission phenomenon. We used the finite-difference time-domain method to design the transmission and the localized surface plasmon resonance electric field distribution in the near field. The focused ion beam method was used to fabricate the nanoholes. The transmittance in the far field was measured by a scanning spectrophotometer. The difference between the design and the experimental results may be caused by the conversion between the near field and the far field. The near field electric field distribution on the surface plasmonic nanoholes was measured by a near-field scanning optical microscope. From our results, we found that the maximum transmission of the nanoholes is 2.4. Therefore, our plasmonic nanohole can significantly enhance the transmission by exciting the plasmonic phenomenon on the surface of the nanostructures.

S. Zhu (✉) · W. Zhou
School of Mechanical and Aerospace Engineering, Nanyang Technological University, 50 Nanyang Avenue, Singapore 639798, Singapore
e-mail: s.zhu2@uq.edu.au

W. Zhou
e-mail: wzhou@cantab.net

Keywords Plasmonic properties · Surface plasmon · Finite-difference and time-domain · Pentagram nanoholes · Focused ion beam

Introduction

In the past decade, many researchers have focused on the fundamental properties, fabrication, and utilization of metal nanostructures. Metal nanoparticles array have high extinction and scattering coefficients which are important for sensitive chemical and biological detection and the development of robust microelectronic devices (Liang et al. 2005; Zhu et al. 2009). In recent years, researchers have discovered localized surface plasmon resonance (LSPR) phenomena (Rindzevicius et al. 2005), and enhanced transmission through metallic sub-wavelength periodic structures (Ebbesen et al. 1998). LSPR has shown great promise to significantly increase the size of the detection array, supporting high throughput applications (Zhu et al. 2008; Leebeeck et al. 2007). The extraordinary optical transmission properties of regular arrays of nanoholes in thin metal films were first reported in 1998 by Ebbesen and his co-workers (Ebbesen et al. 1998; Ctistis et al. 2007). The similarities between the LSPRs of nanoholes and nanodisks were discussed by Haynes et al. (2003). Periodic arrays of cylinder-shaped nanoholes exhibit more complex behavior than the isolated nanoholes (Yin et al. 2004), with light transmission peaks exhibiting distinct minima and maxima that can be very well

described with Fano lineshape models. This behavior is correlated with the coupling of SPP Bloch waves and more directly transmitted waves through the holes (Chang et al. 2005). The surface plasmon resonance of a square array of rectangular metal-film nanohole arrays was reported by Zhou et al. (2008). Recently, there has been an increased interest in the influence of the hole shape on the transmission properties (Gordon et al. 2005). It was shown that for randomly distributed and periodically arranged rectangular holes, the transmission depends on the aspect ratio of the hole, which was called the "shape-effect" (Koerkamp et al. 2004). It was postulated that the "shape-effect" was the result of localized SP resonances. From these reports, we can deduce that the shape of the nanoholes can affect the transmission and the electric field distribution. The materials, shapes, and the period parameters are important for the nanohole design and their properties.

In this study, we report on the two-dimensional metallic pentagram nanohole array to realize the extraordinary transmission phenomenon. We chose the pentagram nanohole because pentagram has more sharp tips than the traditional ones. The finite-difference time-domain (FDTD) method (Kunz and Luebbers 1993) was used to design and calculate the transmission and the localized electric field distribution. The fundamentals of the FDTD method are to solve Maxwell's curl equations in the time-domain (Taflove 1995). The FDTD is characterized by the solution of Maxwell's curl equations in the time-domain after replacement of the derivatives in them by finite differences. It has been applied to many problems of propagation, radiation, and scattering of electromagnetic waves (Taflove and Hagness 2000). Our designed nanohole arrays were fabricated using the focused ion-beam (FIB) milling method. The optical properties of the nanohole arrays were explored by the spectrometry and the near-field scanning optical microscope (NSOM) system. Both the calculated and experimental results show that the pentagram nanohole array can significantly enhance the localized electric field and the transmission which can be used as a nanobiosensor and in the imaging field in the future.

Design nanoholes using FDTD

In order to derive the plasmonic properties of the pentagram nanohole array, optimization design in terms of Maxwell electromagnetic equations is required. We optimized the design by selecting material parameters (refractive index, extinction coefficient, permittivity, and permeability), wavelength of incident light, dimension, and shape of the nanoholes. Design and simulation of the nanoholes was performed using professional software-three-dimensional FDTD solution. The FDTD has computational advantages of reducing memory requirement and ease in treating complex materials and shapes. Figure 1 shows our designed geometrical model of the Ag pentagram nanohole array. The pentagram nanohole array was arranged in the symmetry two-dimensional infinite arrays. This pentagram nanohole array lied in the x–y plane and the incident light polarized of x axis propagates along z axis. The out-of-plane heights of the Ag nanoholes was 40 nm. The in-plane widths of each nanoholes was 500 nm. The period of the nanohole array was 500 nm, and the refractive index of the medium surrounding the Ag nanohole is 1.0 (in air). For the Ag material, we used Drude model (Yang et al. 2009; Li et al. 2001; Yuan and Shi 2007) to calculate the electronic distribution on the surface of the pentagram nanohole array. For the nanoholes, a glass substrate ($n = 1.52$) was used, the thickness we selected was 1,000 nm which is larger than out-of-plane heights of the Ag.

According to the design model shown in Fig. 1, we calculated the transmission in the z direction and the localized electric field distribution using the FDTD method. The simulation parameters of the FDTD algorithm were set as follows: the incident light ranges from 400 to 1,200 nm with plane wave in the normal

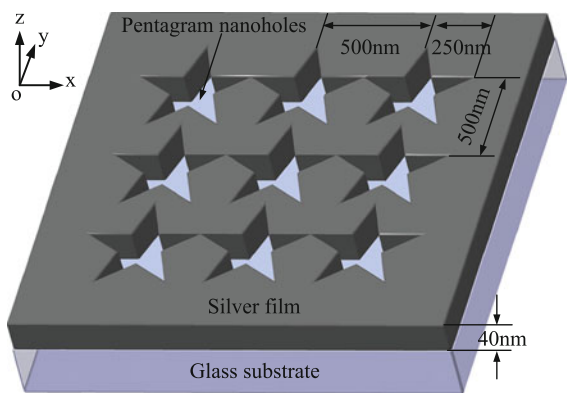

Fig. 1 The symmetry two-dimensional infinite model of Ag pentagram nanohole arrays

incidence angle $\theta = 0^\circ$. Meshing size in x and y (two-dimensional simulation) is $\Delta x = 2$ nm and $\Delta y = 2$ nm, respectively. Simulation time t (theoretically, $t = \Delta x/2c$, c is the velocity of light) was set to be 125 fs. The output result is the relationship between the transmission and the incident wavelength. Figure 2 shows the transmission of the pentagram nanohole arrays calculated by the FDTD method. From Fig. 2, we can see that the peaks of the transmission in the z direction are 458.687, 542.466, 633.687, and 854.676 nm. The transmissions of these peaks are higher than 1 which is the maximum transmission in the traditional optical field. The maximum transmission of the nanoholes is 2.4. This result indicated that our designed plasmonic nanohole can significantly enhance the transmission by exciting the plasmonic phenomenon on the surface of the nanostructures.

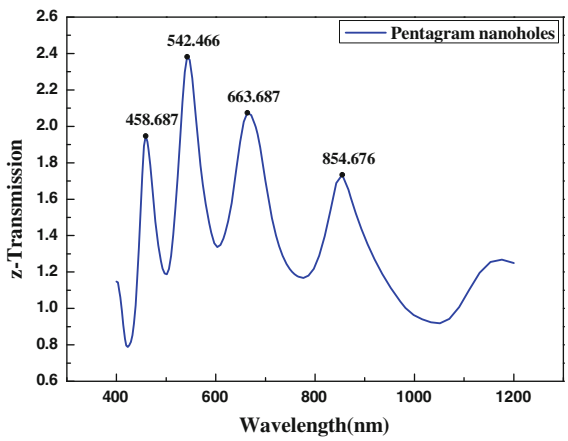

Fig. 2 The transmission of the pentagram nanohole arrays calculated by FDTD

In order to fully understand the optical response of our nanohole arrays, we carried out the numerical simulation of the localized electric field (E-field) distribution on the surface of the nanoholes. E-field distributions at x–y, y–z, and x–z planes are shown in Fig. 3a–c, respectively. From Fig. 3, we can see that there is a significant field enhancement at the metal–air interface in the regions between the holes. This phenomenon is consistent with the demonstration of the excitation of surface plasmon-polaritons (SPP) of the metal film in the vicinity of the nanoholes (Sonnichsen et al. 2000). The E-field distribution is asymmetric because of the illumination of the TM mode linear polarization. The field enhancement between the holes in Fig. 3b, c suggests that our nanohole arrays, nearly symmetric SPPs supported by the metal film may play an important role in determining the response. For example, the Ag film connecting adjacent pentagram nanoholes could provide an additional coupling sites between the localized resonances of the nanoholes, and one mediated by nearly symmetric SPPs. The reason is due to the excitation of SPPs through scattering that enables the LSPR modes of adjacent nanoholes to interact sufficiently, so a spectral shift in their response occurs. This phenomenon can be used in the nanobiosensor field in the future.

Results and discussion

Fabrication nanoholes using FIB

The FIB direct milling technique (Nagoshi et al. 2009; Fu et al. 2007; Rommel et al. 2010) is the best option to

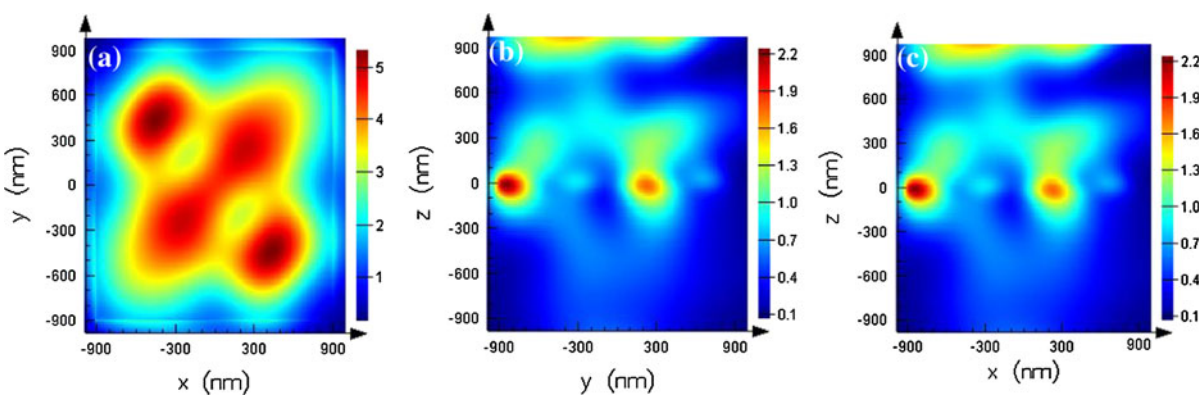

Fig. 3 Localized electronic field distribution in the transmission direction of the Ag pentagram nanohole array calculated by FDTD when the period of the nanostructure array is 500 nm. **a** x–y plane, **b** y–z plane, and **c** x–z plane

fabricate such nanostructures due to its unique advantages of one-step fabrication, nanoscale resolution, no materials selectivity, etc. Ag pentagram nanohole arrays were fabricated by FIB milling (FEI Nova 200 SEM/FIB dual-beam workstation is available for fabrication of the nanostructures). The nanostructure can be directly fabricated using FIB milling on Ag thin film coated onto a glass substrate. At first, the glass substrate was cleaned in a piranha solution (1:3 30% H_2O_2/H_2SO_4) at 80 °C for 30 min, and then the substrate was cooled by high-pressure N_2. Once cooled, the glass substrates were rinsed with copious amounts of distilled water and sonicated for 60 min in 5:1:1 H_2O/NH_4OH/30% H_2O_2. Next, the Ag metal thin film was sputtered on the surface of the glass substrates. Finally, the FIB was used to fabricate the pentagram nanohole arrays. Figure 4 shows a SEM image of the FIB fabrication result. The inset picture is the glass substrate including the nanohole arrays taken by camera. The diameter of the substrate is 25 mm, and the thickness is 2 mm. The FIB fabricate nanohole arrays are in the circle labeled by the blue colored line. From Fig. 4a, we can see that the pentagram nanohole array is milling on the surface of the Ag film directly. The in-plane width of the Ag pentagram nanoholes is around 500 nm, the thickness of the Ag is about 40 nm, and the period of array is approximately 500 nm just as the designed parameters. A SEM image on a larger length scale is provided to demonstrate the integrity of the nanoholes array film as shown in Fig. 4b. The irregular shape error is caused by the FIB nanofabrication method.

Optical properties of the nanoholes

In order to observe the optical properties of the pentagram nanohole arrays, we used spectrometry (UV-3101 PC UV–VIS-NIR Scanning Spectrophotometer) to detect the transmittance of the fabricated pentagram nanoholes. Figure 5 shows the experimental transmittance spectra of the pentagram nanohole arrays, inset is the AFM image of the nanoholes. Interestingly, for the nanohole array, it can be seen in Fig. 5 that the peaks of the transmittance are 565.5, 601, 633.687, and 642.5 nm. The mismatch between the calculated transmission and the experimental transmittance spectra is caused by the different detection positions. For the calculated results, the position is near to the surface of the nanoholes. FDTD software cannot

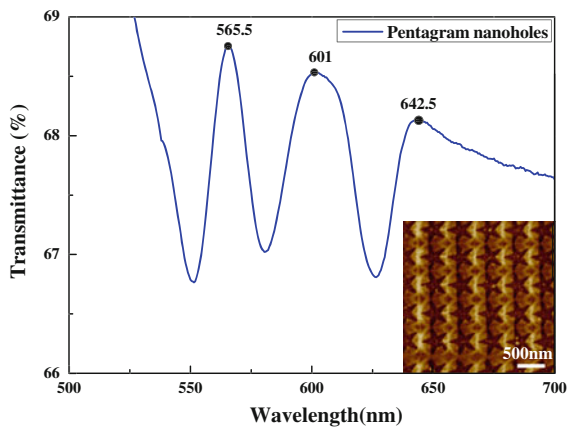

Fig. 5 Experimental transmittance spectra of the pentagram nanohole arrays, *inset* is the AFM image of the nanoholes

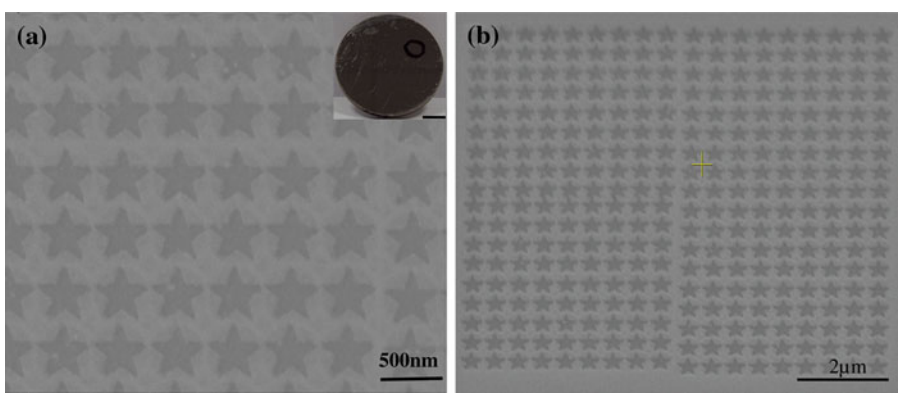

Fig. 4 **a** SEM micrographs of the FIB fabrication result, inset is the glass substrate including the nanohole arrays taken by camera (The *scale bar* for the *inset* photo is 500 μm). **b** SEM image on a larger length scale to demonstrate the integrity of the nanoholes array film

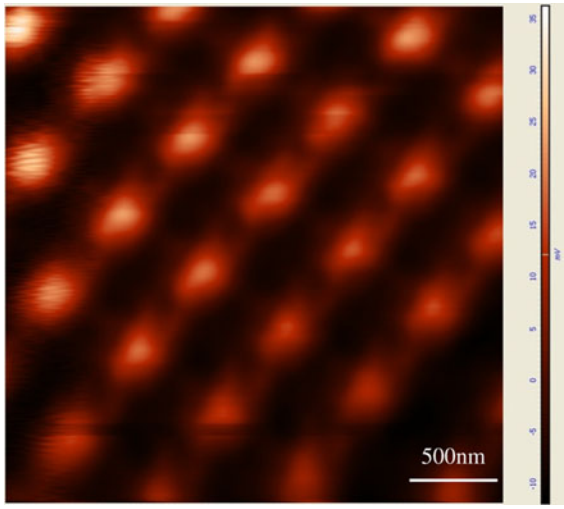

Fig. 6 Localized electric field distributions of nanoholes detected by NSOM system

calculate the far field design. However, in the experimental detection, the CCD camera is far away from the sample because we must use focus lens to guide the light to the detector.

The localized electric field distribution on the surface of the nanoholes array was detected by the NT-MDT NSOM system. Figure 6 indicates the distribution of nanoholes detected by the NSOM system. It is the near field optical intensity distribution of the nanoholes. We selected the transmission mode for the NSOM system to obtain the *E*-field distribution. From Figs. 6 and 3a, we can see that the experimental optical intensity distribution almost correspond to the design result. There are hot-spots for the nanohole array which is caused by the surface plasmon resonance excited by free electrons and the incident light.

Conclusion

We have promoted a pentagram nanohole array to enhance the LSPR. Plasmonic properties of two-dimensional Ag nanoholes were investigated by the FDTD method in theory design. The calculated results indicate that the maximum transmission of the nanoholes is 2.4 times higher than the maximum of the traditional transmission. In the experimental part, we fabricated the nanoholes by FIB lithography. The transmittance and the localized electric field distribution of the nanoholes were detected by spectrometry and the NSOM system. The detection results show that our proposed nanoholes can significantly enhance the transmission and *E*-field. The nanoholes have potential applications in imaging, focusing, and nanobiosensor fields.

Further investigations concerning the relationship between the transmission in the near field and the far field of nanoholes with different diameters and interhole distance are currently being designed and prepared.

Acknowledgments This study was supported by the A*STAR (Agency for Science, Technology, and Research), Singapore, under SERC Grant No. 0721010023.

References

Chang SH, Gray S, Schatz G (2005) Surface plasmon generation and light transmission by isolated nanoholes and arrays of nanoholes in thin metal films. Opt Express 13(8): 3150–3165. doi:10.1364/OPEX.13.003150

Ctistis G, Patoka P, Wang X, Kempa K, Giersig M (2007) Optical transmission through hexagonal arrays of sub-wavelength holes in thin metal films. Nano Lett 7: 2926–2930. doi:10.1021/nl0712973

Ebbesen TW, Lezec HJ, Ghaemi HF, Thio T, Wolff PA (1998) Extraordinary optical transmission through sub-wavelength hole arrays. Nature 391:667–669. doi:10.1038/35570

Fu YQ, Zhou W, Lim LEN, Du C, Shi H, Wang CT, Luo X (2007) Influence of V-shaped plasmonic nanostructures on beam propagation. Appl Phys B 86:461–466. doi:10.1007/s00340-006-2502-9

Gordon R, Hughes M, Leathem B, Kavanagh KL, Brolo AG (2005) Basis and lattice polarization mechanisms for light transmission through nanohole arrays in a metal film. Nano Lett 5:1243–1246. doi:10.1021/nl0509069

Haynes CL, McFarland AD, Zhao L, Van Duyne RP, Schatz GC, Gunnarsson L, Prikulis J, Kasemo B, Käll M (2003) Nanoparticle optics: the importance of radiative dipole coupling in two-dimensional nanoparticle arrays. J Phys Chem B 107:7337–7342. doi:10.1021/jp034234r

Koerkamp KJK, Enoch S, Segerink FB, van Hulst NF, Kuipers L (2004) Strong influence of hole shape on extraordinary transmission through periodic arrays of sub-wavelength holes. Phys Rev Lett 92:183901. doi:10.1103/PhysRevLett.92.183901

Kunz KS, Luebbers RJ (1993) The finite difference time domain method for electromagnetics. CRC Press, Boca Raton

Leebeeck AD, Kumar LKS, de Lange V, Sinton D, Gordon R, Brolo AG (2007) On-chip surface-based detection with nanohole arrays. Anal Chem 79:4094–4100. doi:10.1021/ac070001a

Li HY, Zhou SM, Li J, Chen YL, Wang SY, Shen ZC, Chen LY, Liu H, Zhang XX (2001) Analysis of the drude model in

metallic films. Appl Optics 40(34):6307–6311. doi:10.1364/AO.40.006307

Liang Y, Zhai L, Zhao X, Xu D (2005) Band-gap engineering for semiconductor nanowires through composition modulation. J Phys Chem B 109:7120–7123. doi:10.1021/jp045566e

Nagoshi K, Honda J, Sakaue H, Takahagi T, Suzuki H (2009) Direct fabrication of nanopores in a metal foil using focused ion beam with in situ measurements of the penetrating ion beam current. Rev Sci Inst 80:125102. doi:10.1063/1.3270958

Rindzevicius T, Alaverdyan Y, Dahlin A, Höök F, Sutherland D, Käll M (2005) Plasmonic sensing characteristics of single nanometric holes. Nano Lett 5:2335–2339. doi:10.1021/nl0516355

Rommel M, Jambreck JD, Ebm C, Platzgummer E, Bauer AJ, Frey L (2010) Influence of FIB patterning strategies on the shape of 3D structures: comparison of experiments with simulations. Microelectron Eng 87:1566–1568. doi:10.1016/j.mee.2009.10.054

Sonnichsen C, Duch AC, Steininger G, Koch M, von Plessen G, Feldmann J (2000) Launching surface plasmons into nanoholes in metal films. Appl Phys Lett 76:140–142. doi:10.1063/1.125682

Taflove A (1995) Computational electrodynamics: the finite-difference time-domain method. Artech House, Boston

Taflove A, Hagness S (2000) Computational electrodynamics: the finite-difference time-domain method, 2nd edn. Artech House, Boston

Yang JS, Lee SG, Park SG, Lee EH, O BH (2009) Drude model for the optical properties of a nano-scale thin metal film revisited. J Korean Phys Soc 55(6):2552–2555. doi:10.3938/jkps.55.2552

Yin L, Vlasko-Vlasov VK, Rydh A, Pearson J, Welp U, Changc S-H, Gray SK, Schatz GC, Brown DB, Kimball CW (2004) Surface plasmons at single nanoholes in Au films. Appl Phys Lett 85:467–469. doi:10.1063/1.1773362

Yuan ZC, Shi JM (2007) Collisional, nonuniform plasma sphere scattering calculation by FDTD employing a Drude model. Int J Infrared Milli Waves 28:987–992. doi:10.1007/s10762-007-9273-1

Zhou RL, Chen XS, Wang SW, Lu W, Zeng Y, Chen HB, Li HJ, Xia H, Wang LL (2008) The surface plasmon resonance of metal-film nanohole arrays. Solid State Commun 145(1–2):23–28. doi:10.1016/j.ssc.2007.10.006

Zhu SL, Li F, Luo XG, Du CL, Fu YQ (2008) A localized surface plasmon resonance nanosensor based on rhombic Ag nanoparticle array. Sens Actuators B 134:193–198. doi:10.1016/j.snb.2008.04.028

Zhu SL, Du CL, Fu YQ (2009) Detection of staphylococcus aureus enterotoxin B using localized surface plasmon resonance-based hybrid Au-Ag nanoparticles. Opt Mat 31:1608–1613. doi:10.1016/j.optmat.2009.03.009